$$\ln(p_{Ni}) = 18.34 - \frac{51\,500}{T} - 0.364 \ln T \qquad (20)$$

(iv) The latent heat of vaporization was taken as: 1.7×10^3 cal g^{-1}.

Noting the definition of Gr, substitution of these quantities into equation (16) gave Nusselt numbers of 2·9 and 3·1, corresponding to surface temperatures of 1500 and 2400°C respectively. In view of this small variation of Nu with temperature in this instance, a mean value of $\overline{Nu} = 3.0$ was used throughout in the calculations.

Finally, it is readily seen by the comparison of equations (12) and (20) that the value of the constant C is given approximately at 51 500 deg K^{-1}.

2 *Calculation of practical values of the Sherwood number*

Practical values of the Sherwood number shown in Fig. 1 have been calculated from the equation:

$$Sh = \frac{h_D d}{\rho_{ef} D}. \qquad (21)$$

Since both iron and nickel evaporate from the surface of the metal drops, the mass-transfer coefficient has been calculated from the equation:

$$h_D = \frac{\dot{m}''}{(m_{Ni})_w + (m_{Fe})_w}. \qquad (22)$$

Where $\dot{m}''$ is the practically measured total evaporation rate, and $(m_{Ni})_w$ and $(m_{Fe})_w$ are the equilibrium mass fractions of nickel and iron in the gas phase in contact with the metal surface. These values have been calculated from the equilibrium data presented by Kubaschewski and Evans [8], and the activity coefficient data presented Hultgren *et al.* [9]. The values of $d/\rho_{ef}D$ has been calculated from the density values determined from equation (19) and diffusion coefficient data presented by Turkdogan [2].

REFERENCES

1. D. E. ROSNER, Enhancement of diffusion limited vaporization rates by condensation within the thermal boundary layer, *Int. J. Heat Mass Transfer* **10**, 1267 (1967).
2. E. T. TURKDOGAN, The theory of enhancement of diffusion limited vaporization rates by convection—condensation process, *Trans. Am. Inst. Chem. Engrs* **230**, 740 (1964).
3. E. T. TURKDOGAN and K. C. MILLS, The theory of enhancement of diffusion limited vaporization rates by convection—condensation process, *Trans. Am. Inst. Chem. Engrs* **230**, 750 (1964).
4. G. W. TOOP, Reactions between gases and levitated metals, Ph.D. Thesis, University of London (1964).
5. A. W. D. HILLS and J. SZEKELY, Notes on vaporization into very much colder surroundings, *Chem. Engng Sci.* **17**, 79 (1964).
6. E. G. BENNETT and J. E. MYERS, *Momentum, Heat and Mass Transfer*, p. 345. McGraw-Hill, New York (1962).
7. E. R. ECKERT and R. M. DRAKE, *Heat and Mass Transfer*. McGraw-Hill, New York (1959).
8. O. KUBASCHEWSKI and E. L. EVANS, *Metallurgical Thermochemistry*. Pergamon Press, London (1956).
9. R. HULTGREN, R. L. ORR, P. D. ANDERSON and K. K. KELLY, *Selected Values of Thermodynamic Properties of Metals and Alloys*. John Wiley, New York (1963).

Int. J. Heat Mass Transfer. Vol. 12, pp. 114–118. Pergamon Press 1969. Printed in Great Britain

THERMAL TURBULENCE CHARACTERISTICS IN SODIUM–POTASSIUM

L. E. HOCHREITER and ALEXANDER SESONSKE

Department of Nuclear Engineering, Purdue University, Lafayette, Indiana 47907, U.S.A.

(*Received* 18 *March* 1968 *and in revised form* 17 *July* 1968)

NOMENCLATURE

$\bar{T}$, mean temperature [°F];
T_w, extrapolated wall temperature [°F];
T_c, centre line temperature [°F];
T_m, bulk mixing cup temperature [°F];
y, distance measured from the wall [ft];
R_0, radius of the pipe [ft];
$\sqrt{(\overline{\theta'^2})}$, RMS value of temperature fluctuation [°F];
$\sqrt{(\theta'^2_{max})}$, maximum value of RMS temperature fluctuation for one set of data;
U_b, bulk average velocity [ft/s];
$\sqrt{(\overline{u'^2})}$, RMS value of velocity fluctuation [ft/h];
$\sqrt{(u'^2_{max})}$, maximum value of velocity fluctuation for one set of data [ft/h];
$(q/A)_w$, wall heat flux [Btu/h . ft^2];
k, thermal conductivity [Btu/h . ft . °F];
U^*, friction velocity [ft/h];
ν, kinematic viscosity [ft^2/h];

ψ, turbulent intensity [°F];
y^{++}, dimensionless distance from the wall;
η, dimensionless distance from the wall.

INTRODUCTION

HEAT-TRANSFER rates may presently be predicted from integral equations such as Lyon's [1], which depend on the eddy diffusivity ratio. Since the dependency of the eddy diffusivity ratio on various process parameters has not been well established experimentally, the integral equations are not applicable in a general way. Another approach to the same problem is to utilize the statistical theory of turbulence to describe the flow field and convective heat-transfer problem. A step in this approach is to measure the turbulent temperature fluctuations in the flow field and compare them with existing velocity fluctuation and temperature fluctuation data in other fluids to provide some insight into the turbulence structure. This work described is a continuation of that of Rust and Sesonske [2], only a sodium–potassium alloy (NaK-56) is used instead of mercury.

EXPERIMENTAL EQUIPMENT

The test loop was installed in the secondary system of a double-loop facility described by Baker and Sesonske [3], which includes an 8000 lb/h electromagnetic pump for circulation.

As shown in Fig. 1, the heated 56-in long test section, constructed of type 304 stainless steel seamless tubing (1·0-in I.D. by $\frac{1}{8}$-in wall), is preceded by a 40-in calming section to assure velocity profile development. The heating section, wound with 0·0125-in by $\frac{1}{8}$-in Nichrome resistance ribbon over an $\frac{1}{8}$-in layer of No. 29 zirconium-based Sauereisen cement which acts as both an electrical insulator and thermal diffuser to provide a uniform wall heat flux, is controlled by three separate autotransformers. Circumferential grooves, $\frac{1}{8}$-in by $\frac{3}{32}$-in deep cut into the tube wall at both ends of the heating section, minimized axial conduction. The thermocouple probe mechanism is attached to the end of the heating section.

Since the objective of this study was to measure rapidly changing fluid temperatures due to turbulence effects, a specially designed fast response thermocouple was used similar to that described by Rust and Sesonske [2]. This thermocouple, developed by Mo-Re Inc., Bonner Springs, Kansas, consists of a chromel-P tube, 0·015-in in diameter, swaged around a 0·003-in constantan wire which is coated with Al_2O_3 as an insulating material. The junction is made by first polishing the end of the tube-wire assembly, and then vacuum depositing a 0·6 μ nickel film on the very end of the polished assembly.

The response time of the thermocouple for a step input of temperature was calculated to be 5·5 ms for water and 0·63 ms for NaK-56, which compares with a measurement in water of 4 ms [4].

EXPERIMENTAL RESULTS

Experimental conditions for each run are shown in Table 1.

Mean temperature profiles are shown in Fig. 2, where the ordinate is a normalized temperature defined as

$$T_{\text{norm}} = \frac{T_w - \bar{T}}{T_w - \bar{T}_c}$$

where T_w is the extrapolated wall temperature, and $\bar{T}_c$ is the centerline temperature which is the minimum temperature of the profile. The abscissa is a normalized radius, $\eta = y/R_0$, where $\eta = 0$ at the bottom of the tube and $\eta = 2$ at the top. All traverses were taken in a vertical plane to detect mean profile distortion, possibly as a result of free convection.

In determining the wall temperature, T_w, it was assumed that the probe measurement closest to the wall was at a distance of one-half the probe diameter, or 0·0075 in. To find the wall temperature, the mean profile was then extrapolated to the wall utilizing,

$$(q/A)_w \frac{1}{k} = \left(\frac{\mathrm{d}\bar{T}}{\mathrm{d}\eta}\right)_{\eta=0}$$

where $(q/A)_w$ is the measured average wall heat flux for each individual run.

The spatial distribution of the RMS temperature fluctuations is shown in Fig. 3.

DISCUSSION

The mean temperature profiles, shown in Fig. 2, compare favorably with those of Schrock [5] measured in the same test section with a "slow" thermocouple. The RMS temperature fluctuation results, shown in Fig. 3, show variation in the fluctuation amplitude exists about the center line, probably due to unequal local wall heat fluxes resulting from small differences in the Sauereisen thickness around the tube. Isakoff and Drew [6] noticed that microscopic differences in local insulation and thermocouple mounting caused different circumferential wall temperatures at one axial location. This same effect was observed by Wilmer [7] on the present test section when it was instrumented with wall thermocouples.

The temperature fluctuation amplitudes, in Fig. 3, do not follow a consistent trend with increasing Reynolds number. A decrease in amplitude with an increase in Reynolds number is expected since the fluid element would be in the neighborhood of the wall for a shorter time and would have less heat transferred to it. This behavior was found experimentally by Subbotin [8] for the Reynolds number range of 20000–200000 in mercury and by Rodriguez–Ramirez [9] for air. Laufer [10, 11] has also shown that the fluctuating velocity components decrease as the Reynolds number increases.

Rust and Sesonske's [2] temperature fluctuation data in mercury, however, also did not show a consistent trend with increasing Reynolds number. They found that the amplitude of the fluctuations increased in the Reynolds number from 49 500 to 145 000, then decreased from 145 000 to 248 000. Since their mean temperature profiles are skewed, indicating secondary flow, and there were large variations in their wall heat flux for different data runs, their results are not conclusive. On the other hand, Epstein [12], in a study of temperature fluctuations at low Reynolds numbers, 4800–7200, also found a similar inconsistency in the temperature fluctuation amplitude with increasing Reynolds number. This seems to be an area in which more experimental effort is needed, yet, the concept of decreasing fluctuation amplitude with increasing Reynolds number appears to be the most logical.

Subbotin [13], in a more recent paper, measured turbulent temperature fluctuations in mercury over a large Reynolds number range, 5×10^3 to 125×10^3, for different wall heat fluxes. He then attempted to collapse all the data into one curve and normalize out the Reynolds number and wall heat flux effect by plotting ψ/ψ_{max} against y^{++}/y^{++}_{max} where

$$\psi = \frac{\overline{\theta'^2}}{(T_w - T_m)}; \quad y^{++} = \frac{yU^*}{\nu} Pr,$$

and ψ attains its maximum at y^{++}_{max}.

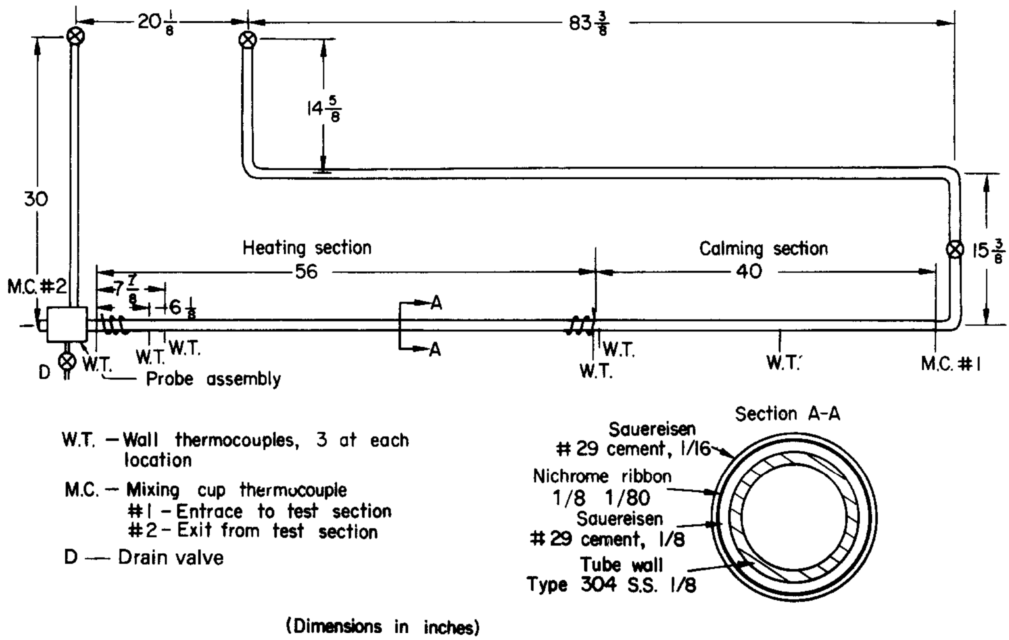

FIG. 1. Schematic of test section. (Dimensions in inches.)

Table 1. Experimental conditions

$T_{b_{inlet}}$ (°F)	$T_{b_{exit}}$ (°F)	U_b (ft/s)	*Re*	$(q/A)_w$ (Btu/h . ft²)	*Pe*	*Nu*†
243·32	256·40	4·2	56 900	11 930	1300	15·0
194·49	214·15	2·8	35 500	12 250	910	12·4
190·12	216·15	2·1	26 800	12 260	690	11·0
155·76	170·81	3·5	41 500	11 870	1160	14·0
164·75	201·98	1·5	18 050	12 270	480	9·6
230·65	241·88	4·9	65 200	12 060	1460	16·0
			Average	12 050		

† Estimated values (±10 per cent) taken from [5].

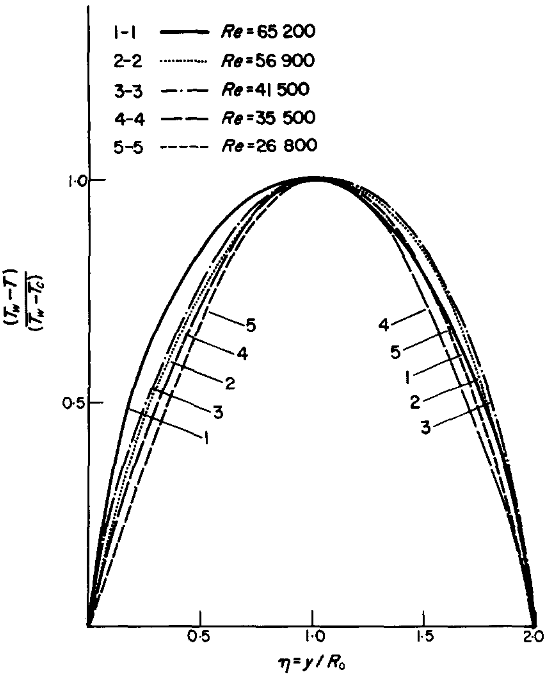

FIG. 2. Mean temperature profiles in NaK.

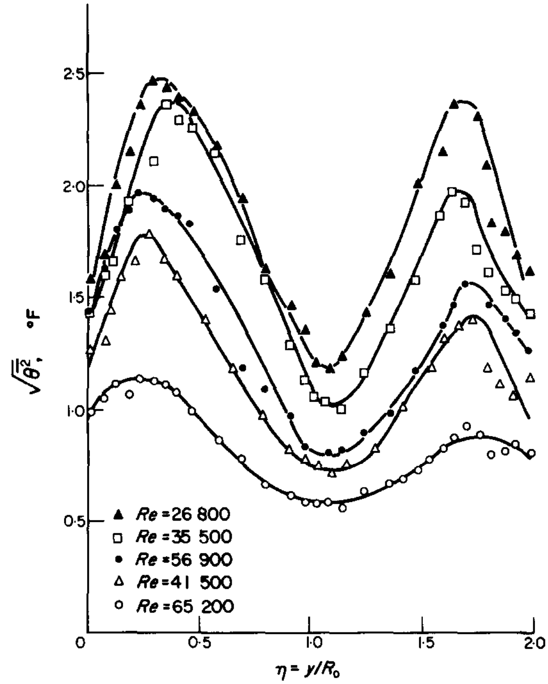

FIG. 3. Temperature fluctuation distributions in NaK.

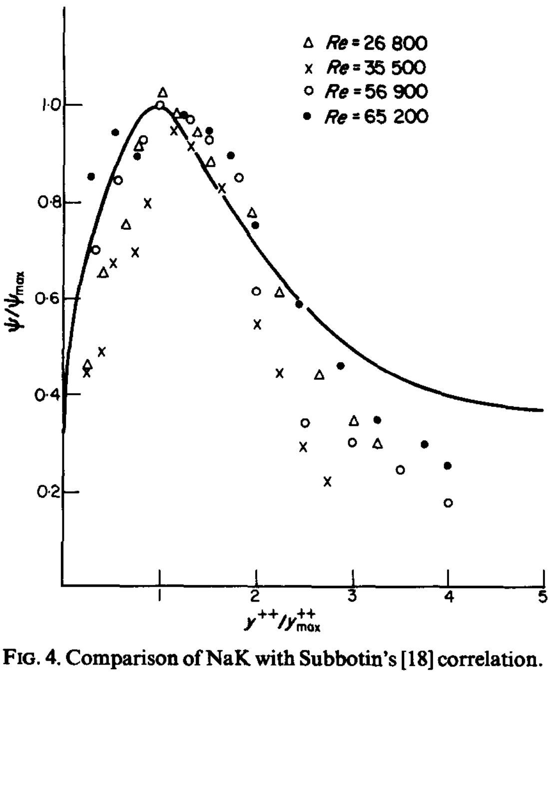

FIG. 4. Comparison of NaK with Subbotin's [18] correlation.

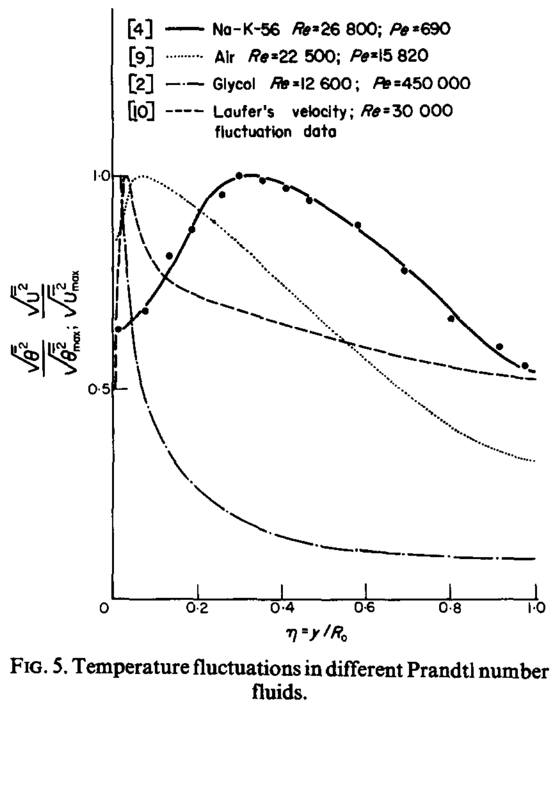

FIG. 5. Temperature fluctuations in different Prandtl number fluids.

The results for sodium–potassium are plotted on Subbotin's curve in Fig. 4. Agreement is fairly good although the present sodium–potassium results generally lie below Subbotin's curve at larger values of y^{++}/y^{++}_{max}. The sodium–potassium results would fit Subbotin's curve slightly better if ψ is defined in terms of the RMS of the turbulent temperature fluctuation rather than the mean square value.

The effect of different fluid Prandtl number on the turbulent temperature fluctuations is shown in normalized form in Fig. 5 with Laufer's [10] velocity data shown for comparison. As the Prandtl number decreases, the molecular conduction effects are enhanced. The region of interplay between the conduction and convection effects therefore dominate the flow field, evident by the broad maximum exhibited in sodium–potassium temperature data, with the opposite true for large Prandtl number fluids such as ethylene glycol. Only in the case of air, with a fluid Prandtl number of 0·704, are the temperature and velocity fluctuation curves similar, as expected from analogy models.

ACKNOWLEDGEMENT

The authors are grateful to the National Science Foundation for the financial support that made this research possible.

REFERENCES

1. R. N. LYON, Liquid metal heat-transfer coefficients, *Chem. Engng Prog.* **47**, 75–79 (1951).
2. J. H. RUST and A. SESONSKE, Turbulent temperature fluctuations in mercury and ethylene glycol in pipe flow, *Int. J. Heat Mass Transfer* **9**, 215–227 (1965).
3. R. A. BAKER and A. SESONSKE, Heat transfer in sodium–potassium alloy, *Nucl. Sci. Engng* **13**, 283–288 (1962).
4. L. E. HOCHREITER, Turbulent temperature fluctuations in flowing sodium–potassium, M.S. Thesis, Purdue University (1967).
5. S. L. SCHROCK, Eddy diffusivity ratios in liquid metals, Ph.D. Thesis, Purdue University (1964).
6. S. E. ISAKOFF and T. B. DREW, Heat and momentum transfer in turbulent flow of mercury, in *General Discussion on Heat Transfer*, pp. 405–409. *Inst. Mech. Engrs–Am. Soc. Mech. Engrs, London* (1951).
7. D. L. WILMER, Heat transfer to a liquid metal in turbulent flow through a round tube, M.S. Thesis, Purdue University (1966)
8. V. I. SUBBOTIN, M. Kh. IBRAGIMOV and E. V. NOMOFILOV, Statistical study of turbulent temperature pulsation in a liquid stream, *Teplofiz. Vysok. Temp.* **2**, 59–64 (1964).
9. A. RODRIGUEZ-RAMINEZ, Characteristics of turbulent temperature fluctuations in air, M.S. Thesis, Purdue University (1965).
10. J. LAUFER, Investigation of turbulent flow in a two-dimensional channel, NACA-Report 1053 (1951).
11. J. LAUFER, The structure of turbulence in fully developed pipe flow, NACA-Report 1174 (1954).
12. H. L. EPSTEIN, Characteristics of turbulent temperature fluctuations in ethylene glycol, M.S. Thesis, Purdue University (1965).
13. V. I. SUBBOTIN, YU. I. GRIBANOV, M. KH. IBRAGIMOV, E. V. NOMOFILOV and Y. P. BOBKOV, Measurement of intensity of temperature fluctuations in turbulent flow of mercury in a tube, *Teplofiz. Vysok. Temp.* **3**, 665–668 (1965).

Int. J. Heat Mass Transfer. Vol. 12, pp. 118–120. Pergamon Press 1969. Printed in Great Britain

VIEW FACTOR BETWEEN TWO HEMISPHERES IN CONTACT AND RADIATION HEAT-TRANSFER COEFFICIENT IN PACKED BEDS

NORIAKI WAKAO, KOICHI KATO and NOBUO FURUYA

Department of Chemical Engineering, Yokohama National University, Minami-ku, Yokohama, Japan

(*Received* 20 *April* 1968)

NOMENCLATURE

As is well known, the view factor between two bodies is

- A, surface area of hemisphere [m²];
- A_C, cross sectional area of sphere [m²];
- F_{ij}, view factor from surface i to j;
- $\bar{F}_{12}$, view factor from surface 1 to 2, including the effect of refractory surfaces, see equation (3);
- $\mathscr{F}_{12}$, view factor to allow for interchange between surfaces 1 and 2, see equations (4) and (5);
- h_r, radiation heat transfer coefficient [kcal/m²h °C];
- h'_r, based on A_C, see equation (9);
- p, emissivity of hemisphere;
- Q, rate of heat transfer by radiation [kcal/h];
- T, absolute temperature [°K];